Journal of Hazardous Materials 161 (2009) 815–823

Contents lists available at ScienceDirect

Journal of Hazardous Materials

journal homepage: www.elsevier.com/locate/jhazmat

Dechlorination of chlorinated methanes by Pd/Fe bimetallic nanoparticles

Xiangyu Wang, Chao Chen, Ying Chang, Huiling Liu*

Department of Environmental Science and Engineering, State of Key Laboratory of Urban Water Resource and Environment, Harbin Institute of Technology, Harbin 150090, PR China

ARTICLE INFO

Article history:
Received 14 May 2007
Received in revised form 1 March 2008
Accepted 9 April 2008
Available online 16 April 2008

Keywords:
Pd/Fe bimetallic nanoparticles
Chlorinated methane
Dechlorination

ABSTRACT

This paper examined the potential of using Pd/Fe bimetallic nanoparticles to dechlorinate chlorinated methanes including dichloromethane (DCM), chloroform (CF) and carbon tetrachloride (CT). Pd/Fe bimetallic nanoparticles were prepared by chemical precipitation method in liquid phase and characterized in terms of specific surface area (BET), size (TEM), morphology (SEM), and structural feature (XRD). With diameters on the order of 30–50 nm, the Pd/Fe bimetallic nanoparticles presented obvious activity, and were suited to efficient catalytic dechlorination of chlorinated methanes. The effects of some important reaction parameters, such as Pd loading (weight ratio of Pd to Fe), Pd/Fe addition (Pd/Fe bimetallic nanoparticles to solution ratio) and initial pH value, on dechlorination efficiency were sequentially studied. It was found that the maximum dechlorination efficiency was obtained for 0.2 wt% Pd loading. The dechlorination efficiency was observed to increase with increasing Pd/Fe addition. The optimal pH value for dechlorination reaction of chlorinated methanes was about 7. Kinetics of chlorinated methane dechlorination in the catalytic reductive system of Pd/Fe bimetallic particles were investigated. The dechlorination reaction complied with pseudo-first-order kinetics.

1. Introduction

Chlorinated organic compounds (COCs) are widespread environmental contaminants found both in groundwater and soil, many of which are toxic, persistent and poorly biodegradable to biota. They can accumulate gradually in the environment and turn to be a threat to human and ecosystem long-standingly [1,2]. The remediation of groundwater and soil contaminated by COCs has spurred an extensive concern and is becoming a significant priority. Gillham and co-worker recognized that zero-valent iron could act as a reductant to dechlorinate COCs for the first time in 1994, and proposed that *in situ* permeable reaction wall might be applicable for resolving a wide range of COC contamination problems [3]. The zero-valent iron technology immensely interests a great deal of researchers because of the abundance, low cost and non-toxicity of iron, and is at a critical stage of its developmental process up to the present [4]. Muftikian et al. deposited a second metal such as Ni, Cu, Pt or Pd as a catalyst onto the surface of iron to enhance dechlorination efficiency and speed up dechlorination reaction rate [5–9]. As one of the transition metals, noble metal Pd has void orbit, and can form transitional complex compound with chlorine of COCs. On the surface of Pd/Fe particles there forms a high concentration of reactive phase. Pd plays an essential role in the reaction system as a catalyst. Briefly, the effectiveness of Pd/Fe bimetallic particles was most likely ascribed to the ability of Pd to facilitate hydrogen adsorption. Catalytic reductive dechlorination of COCs by Pd/Fe bimetallic particles follows these steps: (I) the corrosion of iron leads to the emergence of H_2; (II) Pd and H_2 are combined to form a transitional compound $Pd{\cdot}H_2$ with H_2 embedded in Pd crystal lattice; (III) $Pd{\cdot}H_2$ dechlorinates COCs. The reaction could be depicted by Eqs. (1)–(6) and Fig. 1:

$$(I)Fe + 2H^+ \rightarrow Fe^{2+} + H_2 (\text{in acidic solution}) \quad (1)$$

$$Fe + 2H_2O \rightarrow Fe^{2+} + H_2 + 2OH^- (\text{in alkaline solution}) \quad (2)$$

$$Fe + RCl + H^+ \rightarrow RH + Fe^{2+} + Cl^- \quad (3)$$

$$(II)Pd + H_2 \rightarrow Pd{\cdot}H_2 \quad (4)$$

$$Pd + RCl \rightarrow Pd\cdots Cl\cdots R \quad (5)$$

$$(III)Pd{\cdot}H_2 + Pd\cdots Cl\cdots R \rightarrow RH + H^+ + Cl^- + 2Pd \quad (6)$$

In the presence of transitional compound, the dechlorination activation energy is decreased [10–14]. The diameter of Pd/Fe bimetallic nanoparticles is typically less than 100 nm. The surface area of Pd/Fe bimetallic nanoparticles (averagely about 33.5 m^2/g) is notably larger than that of microscale iron powder (usually less than 0.9 m^2/g) [15]. Due to the large surface area and the catalytic function of Pd, Pd/Fe bimetallic nanoparticles possess a high reactivity and effective dechlorination capability. In addition, the nanoscale bimetallic system used for treatment of COCs has

* Corresponding author. Tel.: +86 451 86283008; fax: +86 451 86282103.
E-mail address: liuhl@hit.edu.cn (H. Liu).

0304-3894/$ – see front matter © 2008 Elsevier B.V. All rights reserved.
doi:10.1016/j.jhazmat.2008.04.027

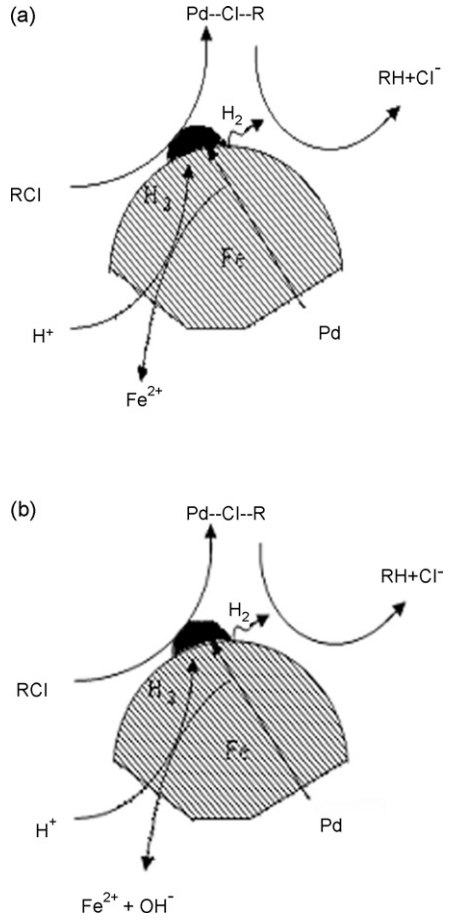

Fig. 1. Scheme of COC catalytic dechlorination by Pd/Fe bimetallic particles: (a) in acidic solution; (b) in basic solution.

unique advantages. Nanoparticles remain suspended in aqueous when being agitated gently. Gravity has little effect on transport and deposition of nanoparticles in porous media, and Brownian motion is the dominative motion of nanoparticles. Accordingly, the superiorities of using bimetallic nanoparticles for environmental remediation include: (1) the nanoparticles may be delivered to deep contamination zones by injection, and (2) bimetallic nanoparticles are more effective at degrading some contaminants [12,14].

Chlorinated methanes are typical and ubiquitous COCs. They are associated with a broad range of industrial or water treatment processes, and exceptionally environmental recalcitrant. Carbon tetrachloride (CT) and chloroform (CF) are applied as solvent in many fields, such as degreasing, cleaning and extracting. Substantial amounts of chlorinated methanes would give rise to ozone depletion when being released into the environment intentionally or inadvertently. The detrimental effects of chlorinated methanes to the environment cannot be overlooked. Therefore, the detoxification of chlorinated methanes becomes a challenging environmental problem. Generally the early researches focused on the dechlorination of many kinds of COCs, such as chlorinated aromatic and olefin hydrocarbons [16–20]. However, the interests have already been aroused to detoxify chlorinated methanes. Song and Carraway dechlorinated CT, CF and dichloromethane (DCM) by using nanosized iron [21]. Lien et al. explored the effects of heavy metals (e.g. Cu, Pb and As) on the dechlorination of CT by iron nanoparticles [22]. Feng and Lim addressed the area of dechlorinating several chlorinated and brominated methanes by nanoscale Pd/Fe bimetallic particles, and suggested that much work should be done to establish robust and versatile liner free energy relationships for reductive dehalogenation of various halogenated aliphatics [23]. This study aimed at assessing the effectiveness of Pd/Fe bimetallic nanoparticles in dechlorinating chlorinated methanes, and the effects of several main parameters, such as Pd loading, Pd/Fe addition, and initial pH value of solution, on dechlorination efficiency. The data from this paper are expected to provide helpful information for the designing of the effective Pd/Fe bimetallic system to treat chlorinated methane contaminated site in a very practical point of view. The dechlorination intermediates and final products were monitored. Furthermore, reaction kinetics and mechanisms of chlorinated methane dechlorination were discussed.

2. Experimental

2.1. Chemicals

The chemicals used were potassium borohydride (KBH_4, 99%), ferric chloride ($FeCl_3{\cdot}6H_2O$, analytic reagent), palladium acetate ($[Pd(C_2H_3O_2)_2]_3$, 47.4 wt% Pd), potassium hydrate (KOH, analytic reagent), methanol (analytic reagent), ethanol (analytic reagent), acetone (analytic reagent), CCl_4 (99.8%), $CHCl_3$ (99.8%), CH_2Cl_2 (99.5%), CH_4 (99.9999%, v/v).

All the chemicals are pure and were used without purification.

2.2. Pd/Fe bimetallic nanoparticles preparation procedure

Nanoscale iron was prepared by adding 30 g of KBH_4 solution dropwise to 1.0 M $FeCl_3{\cdot}H_2O$ solution with vigorous magnetic stirring for complete admixture in an anaerobic glove chamber in an effort to keep O_2 away, otherwise the particles would be oxidized rapidly on the surface. The solution was stirred for additional 5 min after KBH_4 was added to $FeCl_3$ solution. Zero-valent iron could be synthesized according to the following equation:

$$4Fe^{3+} + 3BH_4^- + 9H_2O \rightarrow 4Fe^0\downarrow + 3H_2BO_3^- + 12H^+ + 6H_2\uparrow \quad (7)$$

The iron metal particles were rinsed three times with deionized water and then harvested by vacuum-filtering through a piece of membrane with a pore size of 0.22 μm. No chloride ions were detected in filtrate. Freshly made nanoscale Fe was charged into ethanol solution of palladium acetate. This caused the reduction and deposition of Pd on nanoscale Fe surface. The reaction can be represented as:

$$Pd^{2+} + Fe^0 \rightarrow Pd^0 + Fe^{2+} \quad (8)$$

The Pd/Fe bimetallic nanoparticles were rinsed seriatim with ethanol and acetone till no chloride ions were detected in filtrate, then vacuum-filtered through a piece of polyvinylidene fluoride membrane. The wet freshly prepared Pd/Fe bimetallic nanoparticles were dried in a vacuum oven for 6 h at 100 °C. Next, Pd/Fe bimetallic nanoparticles were restored in vials.

2.3. Characterization of Pd/Fe bimetallic nanoparticles

The BET (Brunauer–Emmett–Teller) surface area of Pd/Fe bimetallic nanoparticles was determined using Autosorb-1 surface analyzer (Quantachrome Instruments, USA) by employing nitrogen adsorption method. The morphology of Pd/Fe bimetallic nanoparticles was viewed with MX2600FE SEM (Camscan Ltd., the UK). Localized Pd/Fe bimetallic information from the chosen region was obtained with INCA EDS (Oxford Instruments, the UK) in conjunction with SEM. The Pd/Fe bimetallic particles size and size distribution were observed with a JEM-1200EX TEM (JEOL Ltd., Japan), and the crystal structure of Pd/Fe bimetallic nanoparticles was examined with a D/Max-rB XRD (Rigaku Corporation, Japan).

2.4. Dechlorination of chlorinated methanes

The stock solution of chlorinated methane was achieved by using methanol as solvent. A chlorinated methane solution of a desired concentration was prepared by spiking a known volume of the stock solution into an aqueous solution. Each batch reaction took place in a serum bottles fitted with a teflon-lined butyl rubber septa crimpstyle cap. In most cases, the bottles containing Pd/Fe bimetallic nanoparticles were filled with solutions containing chlorinated methane, and then sealed immediately with septa. These bottles were placed on a rotary shaker (170 rpm, $22 \pm 1\,^{\circ}C$). For the measurement of chloride ion, liquid samples were taken off from the supernatant using a gastight syringe in the respective reaction vial at the desired sampling times, and then filtered through a piece of membrane filter with a pore size of 0.45 μm. For the measurement of chlorinated methanes and dechlorination intermediates, batch experiments were conducted in 150 mL serum bottles. Each sample bottle was prepared for the chlorinated methane concentration analysis only at each correspondent reaction time. To identify the methane presumably generated during the reaction, batch experiments of dechlorination were repeated with serum bottle and headspace was left in each bottle.

2.5. Analytical method

Chloride ion was analyzed by using 4500i IC (Dionex Corporation, USA). Column size: 4 mm × 250 mm; eluent: 1.7 mM $NaHCO_3$ + 1.8 mM Na_2CO_3 (with chemical suppression); sample size: 20 μL; flow rate: 1.0 mL/min; detector: suppressed conductivity detector. Prior to injection, sample solutions were filtered through a 0.45 μm membrane filter. Dechlorination efficiency was calculated as the ratio of free chloride measured to free chloride ion concentration theoretically produced by the complete dechlorination of chlorinated methane (i.e., dechlorination efficiency = $(C_{Cl^-}/4C_{CT}) \times 100\%$).

Chlorinated methane (CT, CF, and DCM) concentrations were measured by the static headspace gas chromatograph (GC) method. At selected time intervals, a 60 μL headspace aliquot was withdrawn with a gastight syringe from the batch bottle for GC analysis by using HP4890 GC (Agilent Company, USA). The detector is an electron capture detector (ECD). Capillary column is 30 m × 0.32 mm (Agilent). Temperature conditions were set herein as follows: the oven temperature at 65 °C; the injection port temperature at 200 °C; the detector temperature at 300 °C; carrier gas for GC was ultra-pure nitrogen at a flow rate of 5 mL/min. The retention time of CT, CF and DCM was 3.9, 3.2 and 2.5 min, respectively. The detection limits for the chlorinated methanes were between 2 and 5 μL/L.

As for methane measurement, vials with aqueous samples from batch bottles were equilibrated at 25 °C for 6 h. Headspace samples (100 μL) were withdrawn with a gastight syringe and measured by using HP4890 GC equipped with a flame ionization detector (FID) and an AT-Q column. The constant temperatures of the oven, injection, and detector were set at 85, 200, and 300 °C, respectively.

3. Results and discussion

3.1. Characterization of Pd/Fe bimetallic particles

3.1.1. Specific surface area, size, and morphology of Pd/Fe bimetallic nanoparticles

Surface area is taken into account by evaluating the reactivity of nanoparticles and calculating the normalized dechlorination reaction rate constant. More reactive sites are provided when available surface area is increased, thus the effectiveness of the bimetallic system is enhanced. Furthermore, the specific surface area is an important factor of reaction rate and has significant impact on the kinetics of the system. In order to have an in-depth treatment of the pseudo-first-order model, Tratnyek et al. introduced this parameter for the first time in their study. Reaction rate constant can be normalized using the specific surface area [28]. Pristine Pd/Fe bimetallic nanoparticles of this work were found to have a BET specific surface area of 51.4 m^2/g. This resulting value is appreciably higher than those reported ones, and it appears that the synthesis methodology and conditions of nanoparticles might cause the large deviation of their surface areas. In comparison, nanoscale zero-valent iron has a typical BET surface area of about 31.4–36.5 m^2/g accordingly based on the literature [14,24–27]. Liu et al. stated total surface area of Pd/Fe particles was larger than Fe particles and increased with the bulk loading of Pd [7]. The information revealed herein coincides with the abovementioned assertion.

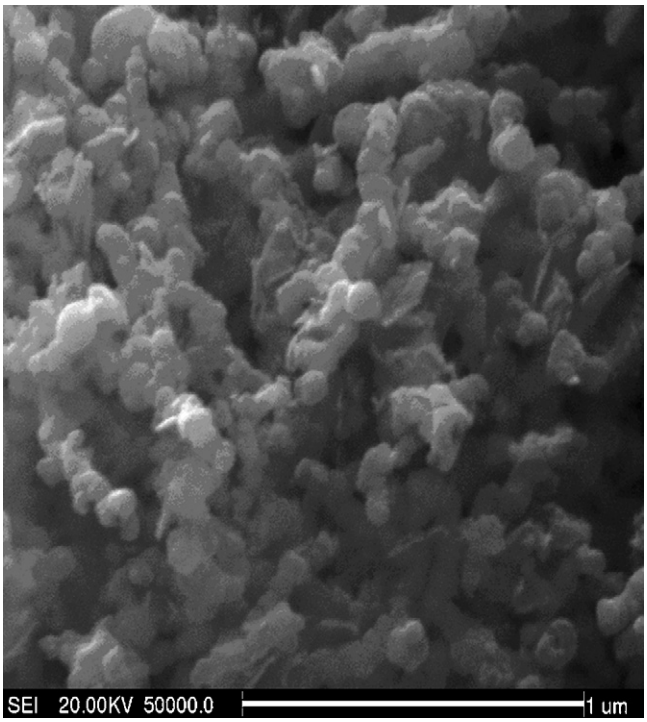

Fig. 2. SEM image of Pd/Fe bimetallic nanoparticles.

The SEM image of Pd/Fe bimetallic nanoparticles is shown in Fig. 2. It could be observed that nanoparticles were roughly spherical and aggregated each other; their diameter ranged from 30 to 50 nm. The morphology of dendritic and chainlike Pd/Fe nanoparticles supports the observation of morphology of iron nanoparticles shown in previous studies [22]. As the dechlorination reaction was considered to take place in the surface of the Pd/Fe bimetallic particles, the coarse and rough morphology of Pd/Fe bimetallic nanoparticle could provide more reactive sites than the smooth morphology, and thereby, was in favor of the dechlorination reaction [6].

The well dispersion degree of Pd on the surface of Pd/Fe bimetallic nanoparticles can advantageously affect the dechlorination reaction. Pd is capable to promote dechlorination reaction in two ways: (1) adsorbing hydrogen and accelerating the dissociation of chlorinated hydrocarbons, (2) preventing iron from being oxidized, especially since Fe particles are known to be active. During the process of dechlorination, H_2 adsorbed by Pd is dissociated into

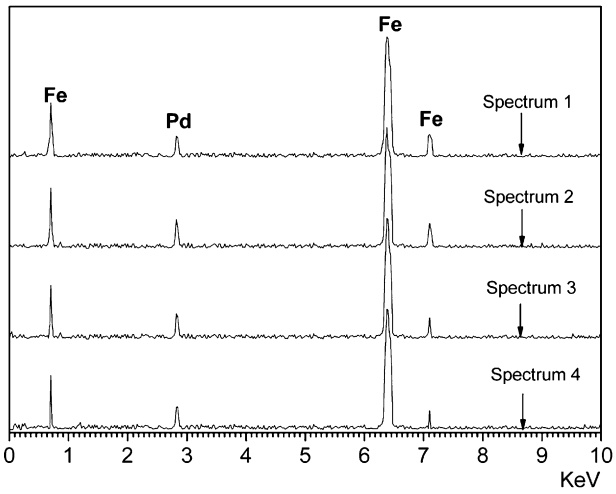

Fig. 3. EDS patterns of Pd/Fe bimetallic nanoparticles.

atomic H, which is one of the strongest reductants, and thereafter chlorine of COCs is replaced by the atomic H [7]. If Pd was poorly dispersed on iron nanoparticles, such as some Pd were overlapped, then not all Pd nanoparticles could be made full use of as catalyst, and therefore the above two roles of Pd cannot be carried out effectively.

Fig. 3 is the localized elemental information of Pd/Fe bimetallic nanoparticles. The EDS analysis profile reveals that Pd distributed and attached to the iron surface evenly and noncontinuously. Metrical Pd loadings of four randomly chosen regions were in the range of 0.19–0.24 wt%. The realistic Pd loadings are close to theoretic Pd loading 0.2 wt%.

In the previous report, Pd was concentrated and mainly coated on the surface of nanoscale iron particles, and the surface content of Pd was higher than the theoretical Pd content [23]. In comparison, a presumption can be deduced from the SEM-EDS spectrum presented in this study that Pd was dispersed rather than forming clusters on the iron particles. A possible explanation for this phenomenon could be partly associated with the efficient mixing of nanoscale iron particles in the ethanol solution of palladium acetate during the preparation of Pd/Fe bimetallic particles to some extent.

The TEM image of Pd/Fe bimetallic nanoparticles exhibits an average particle diameter of approximately 30–50 nm (Fig. 4). The forming of chains is likely due to magnetic interactions between the metallic particles and the natural tendency to remain in the more thermodynamically stable state [29]. The nanosized particles, with diameter in the range of 1–100 nm, resulted in high levels of stepped surfaces that increased their reactivity [30,31].

3.1.2. Structural feature of Pd/Fe bimetallic nanoparticles

The three characteristic peaks of iron metal that appeared at 44.66°, 65.16°, and 82.36° in XRD pattern of Pd/Fe bimetallic nanoparticles were Fe-1 1 0, Fe-2 0 0 and Fe-2 1 1 diffraction peaks, respectively (Fig. 5). The crystal structure of iron was a regular bcc α-Fe crystalline state. No characteristic diffraction peaks of Fe_2O_3 and Fe_3O_4 that indicated the oxidation of zero-valent iron were found. The major surface species of freshly prepared nanoscale Pd/Fe is Fe^0. The diameter of the Pd/Fe bimetallic nanoparticles calculated by Scherer's equation was 38.44 nm. Due to the extreme small Pd content (0.2 wt%) of Pd/Fe bimetallic nanoparticles, no characteristic peaks of Pd appeared in Fig. 5. Nevertheless, Pd particles that deposited onto the iron surface were deemed to be in the form of nanoparticles [32].

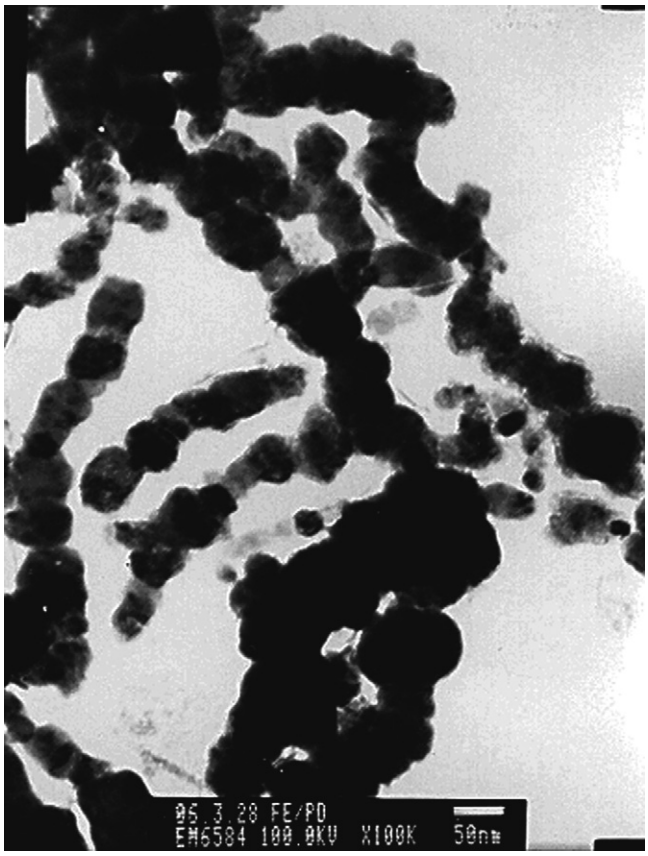

Fig. 4. TEM image of Pd/Fe bimetallic nanoparticles.

3.2. Dechlorination of chlorinated methanes

3.2.1. Effect of Pd loading on dechlorination efficiency

Bimetallic nanoparticles can be prepared using two methods: (1) consecutive reduction of the second metal ions and subsequent deposition onto the first metal particles, and (2) simultaneous reduction of two metal ions. The former method results in the formation of core/shell structure nanoparticles, while the latter method causes the formation of alloy structure nanoparticles [33,34]. Mandal et al. claimed that an average molar ratio of the two metals in the core region was different with that in the shell region, and the result indicated that presence of core/shell structure nanoparticles prepared using the former method [35]. In this experiment, Pd/Fe bimetallic nanoparticles were prepared by the reduction of Pd^{2+} over iron, providing an indication of the core/shell

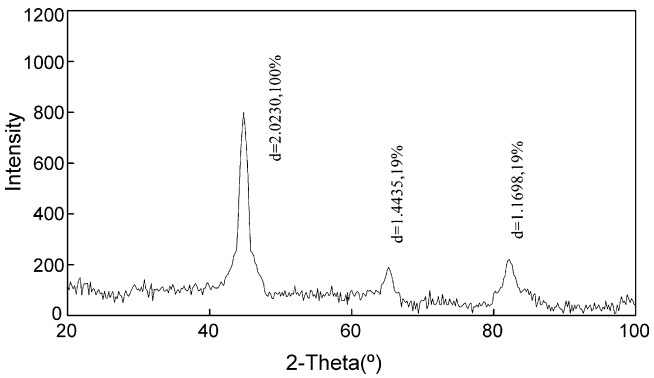

Fig. 5. XRD pattern of Pd/Fe bimetallic nanoparticles.

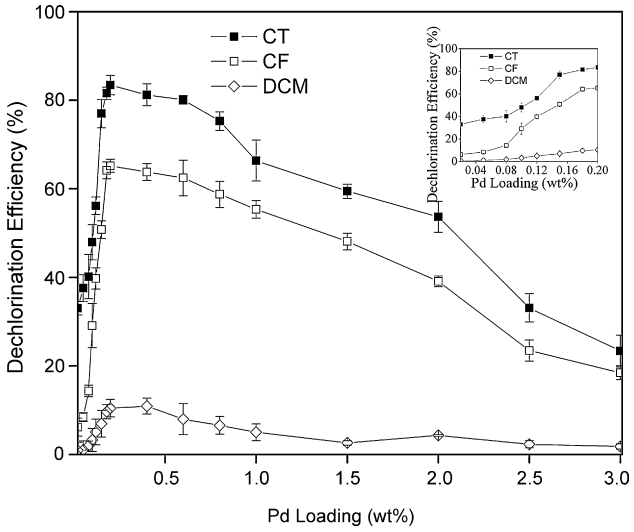

Fig. 6. Effect of Pd loading on dechlorination efficiency (Pd/Fe addition was 10 g/L, initial concentration of chlorinated methane was 100 mg/L, and reaction time was 180 min).

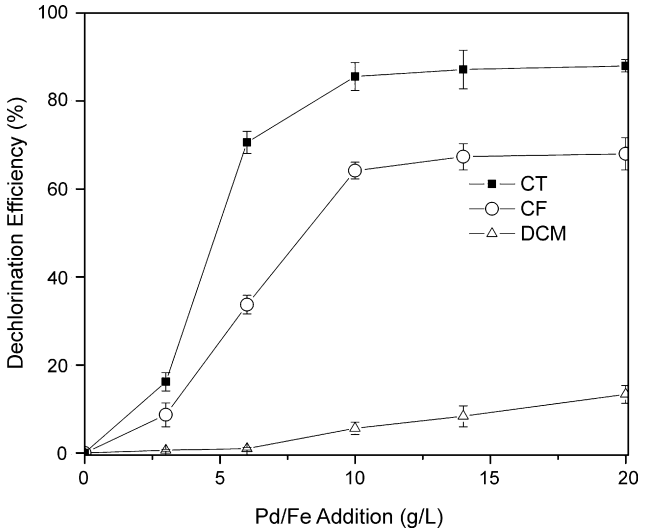

Fig. 7. Effect of Pd/Fe addition on dechlorination efficiency (Pd loading was 0.2 wt%, initial concentration of chlorinated methane was 100 mg/L, and reaction time was 180 min).

structure of achieved Pd/Fe bimetallic nanoparticles. Based on this deduction, the effect of Pd loading on dechlorination of chlorinated methanes cannot be neglected.

The addition of Pd to nanoscale iron particles enables the dechlorination rate increasing rapidly, but it also incurred the increase of the treatment cost. Therefore, finding the lowest level of Pd loading that can be still effective to dechlorinate COCs is economically desirable [25]. Fig. 6 demonstrates that the dechlorination efficiency is dependent on Pd loading. It is clearly observed that as the Pd loading increased, so did the dechlorination efficiency when Pd loading was less than 0.2 wt%. The relatively high dechlorination efficiency could be obtained when Pd loading increased to around 0.20 wt%. In Grittini's hypothesis, the dechlorination of COCs occurs once they are adsorbed on the Pd/Fe surface. Pd on zero-valent Fe surface plays the role of a collector of hydrogen gas that results from the corrosion of Fe [10]. Other researchers have well documented the effect of the loading of the second metal on dechlorination [36,37]. An increase in catalytic metal (e.g. Pd, Ag, or Ni) content with bimetallic particles (e.g., Ag/Fe, Ni/Fe, and Pd/Fe) could promote the iron oxidation and consequently the rate and extent of dechlorination. A higher catalytic metal loading could increase the number of catalytic metal 'islands' (i.e., galvanic cells) and/or the total cathodic areas on the iron surface.

Interestingly, the experimental data showed that increased Pd loading resulted in decreased dechlorination efficiency when Pd loading was more than 0.20 wt%. The increased amount of Pd coating on Fe^0 might hinder the formation of H_2 by Fe^0 corrosion. Dechlorination reaction depended on an active iron surface, and presumably the number of active sites on the surface was not large enough for effective dechlorination, thus the dechlorination efficiency decreased when Pd loading was more than 0.20 wt%.

3.2.2. *Effect of Pd/Fe bimetallic nanoparticles addition on dechlorination efficiency*

It can be ascertained from Fig. 7 that the dechlorination efficiency varied with Pd/Fe additions (3, 5, 10, 14, and 20 g/L). High dechlorination efficiencies of CT and CF could be obtained within 180 min when Pd/Fe addition was 10 g/L (near 80%). Note that the dechlorination efficiency of DCM altered inconspicuously and was still considerably low (the dechlorination efficiency had not reached 20% under 20 g/L Pd/Fe addition within 180 min). In light of previously published data, dechlorination efficiency or observed rate constants could increase with the increase the metal addition [21,38]. The increase of Pd/Fe addition would be expected to increase the reactive Fe site concentration and adsorptive Pd concentration simultaneously followed the increase of dechlorination efficiency.

From Fig. 7, the dechlorination efficiency of CT and CF results in a very little increase when Pd/Fe bimetallic nanoparticles addition was higher than 10 g/L. This evidence revealed that the dechlorination efficiency of chlorinated methanes might not be increased unlimitedly with increasing the addition of Pd/Fe bimetallic nanoparticles. Gillham and O'Hannesin confirmed that there has to be contact between the iron surface and COCs in order for the reduction to occur at significant rate [3]. As pointed out by Matheson and Tratnyek, excessive hydrogen suppressed the continuation of both corrosion of iron and reduction reaction of COCs [4]. Similarly, the present investigation suggested that more than enough hydrogen acted as a site blocker, and became the major and limiting factor for the occurrence of dechlorination when the addition was higher than 10 g/L. Thus, 10 g/L Pd/Fe addition is high enough to provide sufficient reactive capacity, and was chosen as optimal metal addition in the following experiments of this study.

3.2.3. *Effect of pH value on dechlorination efficiency*

The pH value of reaction system is known to affect dechlorination of COCs with zero-valent iron by either producing more corrosion (at lower pH) or more passivation (at higher pH) of iron [4,39]. Jeffers et al. indicated that the dechlorination of pentachloroethane and 1,1,2,2-tetrachloroethane at pH 7 and above became most significant [40]. To extrapolate the result to the full range of conditions in water, evaluating the effect of pH on dechlorination efficiency is necessary. In this study, the initial pH value of the system was adjusted with 0.1% sodium hydroxide solution and 0.1% sulfuric acid solution. The result in Fig. 8 suggests that the optimal initial pH value for the dechlorination of CT, CF and DCM by Pd/Fe bimetallic nanoparticles was 7. The effect of the initial pH value on dechlorination might be attributed to the participation of protons during the reaction. At pH 7, more hydrogen was adsorbed by nanoparticles and dissociated into atomic H to join in the dechlorination of chlorinated methanes. In the lower pH value, the corrosion of iron was initiated leading to production of

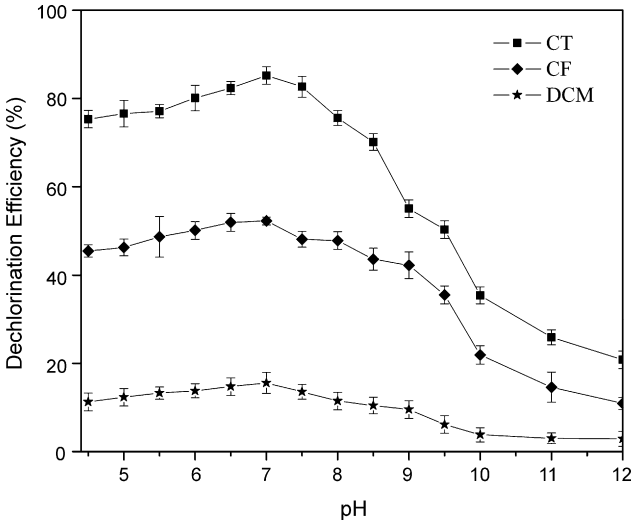

Fig. 8. Effect of pH value on dechlorination efficiency (Pd loading was 0.20 wt%, initial concentration of chlorinated methane was 100 mg/L, Pd/Fe addition was 10 g/L, and reaction time was 180 min).

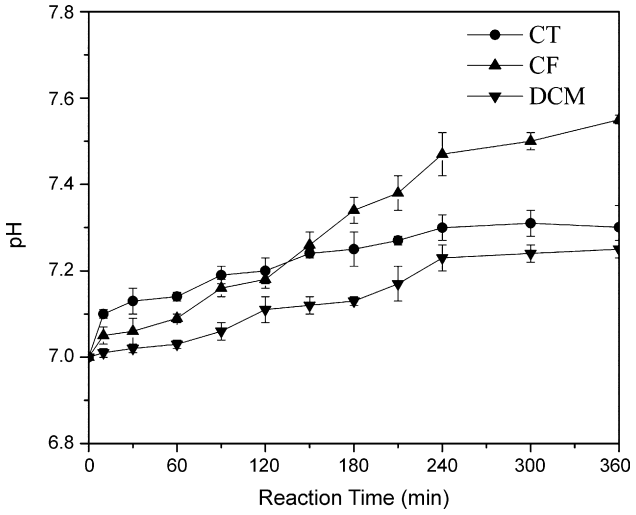

Fig. 9. Change of pH during dechlorination (Pd loading was 0.20 wt%, initial concentration of chlorinated methane was 100 mg/L, and Pd/Fe addition was 10 g/L).

large quantity of H_2 (Eq. (9)), and the minute gas bubbles might act as a barrier to inhibit the contact of particles and target pollutant [4,41–43]. Lowing solution pH expedited the disappearance of zero-valent iron and hence decreased the zero-valent iron concentration [11].

$$Fe^0 + 2H^+ \rightarrow H_2 + Fe^{2+} \quad (9)$$

At pH > 7, the system was lacking in hydrogen indispensable for dechlorination of chlorinated methanes, and the electrons released by iron might be easily obtained by dissolved oxygen in water (Eq. (10)). In alkaline condition, the surface passivating layers formed by the precipitation of metal hydroxides and metal carbonates could likely deactivate Pd/Fe bimetallic nanoparticles [19].

$$O_2 + 2H_2O + 4e^- \rightarrow 4OH^- \quad (10)$$

3.2.4. Change of pH value during the process of dechlorination of chlorinated methanes

Monitoring the pH change over the duration experiment is worthy to be considered for providing a more favorable environment because pH value is liable to evolve in dechlorination. The changes of pH value of the dechlorination reaction solution versus were shown in Fig. 9. The initial pH value of reaction solution was adjusted to 7. Evidently, the changes of pH value were unobvious with the trend of increase by less than 1 unit. The pH value of CT reaction solution increased steadily at first and then became constant, and the change of pH value within 360 min was 0.3. The changing tendency of pH value of CF solution was the same with that of CT. The changes in pH of CF and DCM reaction system in the same time frame were 0.6 and 0.25, respectively. The reasons that result in the change in pH are complicated. The increase of pH value might be attributable to the consumption of H^+ (Eq. (9)). Nonetheless, the reaction shown in Eq. (11) implied a likelihood of the consumption of OH^-. On all accounts, the change of pH value during dechlorination reaction was insignificant.

$$Fe^{2+} + 2OH^- \rightarrow Fe(OH)_2\downarrow \quad (11)$$

3.3. Analysis of intermediates and final products

The identification of intermediate and final product formation of dechlorination of chlorinated methanes is one of the focuses in this study. As depicted in Fig. 10, C denotes the concentration of chlorinated methane, and C_0 denotes the initial concentration of chlorinated methane in the aqueous phase. Blank samples without Pd/Fe bimetallic nanoparticles were used to determine the loss of target pollutant on the basis of its volatilization. The results showed that the volatilized target pollutant was negligible during the reaction, and low-chlorinated methanes underwent dechlorination slower than high-chlorinated methanes in the same reaction conditions (Fig. 10). The reaction rates typically followed the trend of CT > CF > DCM. As for the chlorinated hydrocarbons, increasing the number of chlorine substituents decreases the electron cloud density of carbon atom, and increases the degree of reactivity of getting electron. Thus chlorinated methane with more chlorine atoms would be more prone to be reduced during the process of dechlorination.

Fig. 10(a) reveals that the dechlorination final products and intermediates of CT were CF, DCM, and methane. Concomitant to the dechlorination of CT, methane could be identified immediately after Pd/Fe bimetallic nanoparticles were added to the reaction system. The CF concentrations increased promptly at first, and afterwards decreased slowly after 90 min (<5.58%). The DCM concentrations increased stably and continuously, and remained constant after 60 min. CT might be transformed into methane directly or be dechlorinated to CF and DCM, and then CF was dechlorinated to DCM. According to the decrease of CT concentration, almost 100% of CT was transformed within 180 min. Meanwhile, Cl^- concentration increased, but not all CT was dechlorinated (dechlorination efficiency of CT was 81% within 180 min). The discrepancy could be explained by two reasons: (1) the adsorption of CT on the surface of Pd/Fe bimetallic nanoparticles, which basically caused the result that the amount of determined CT was less than actual amount; (2) the presence of intermediates such as CF and DCM. Specifically, the 77.48% of CT was reduced to CF, DCM and CH_4 in the first 30 min, and 15.98% of CT was reduced in the second 30 min. This phenomenon suggests that intermediate products CF and DCM were more difficult to reduce than CT.

Fig. 10(b) shows that the reduction of CF proceeded rapidly. The major intermediate of the CF dechlorination reaction was DCM. Concomitant to the dechlorination of CF, the concentration of DCM increased gradually and then decreased insignificantly. As a whole, more than 99% of CF was transformed within 240 min. Methane was the major product of the CF dechlorination. It could also hypothesized from Fig. 10(b) that the adsorption of CF on Pd/Fe bimetallic

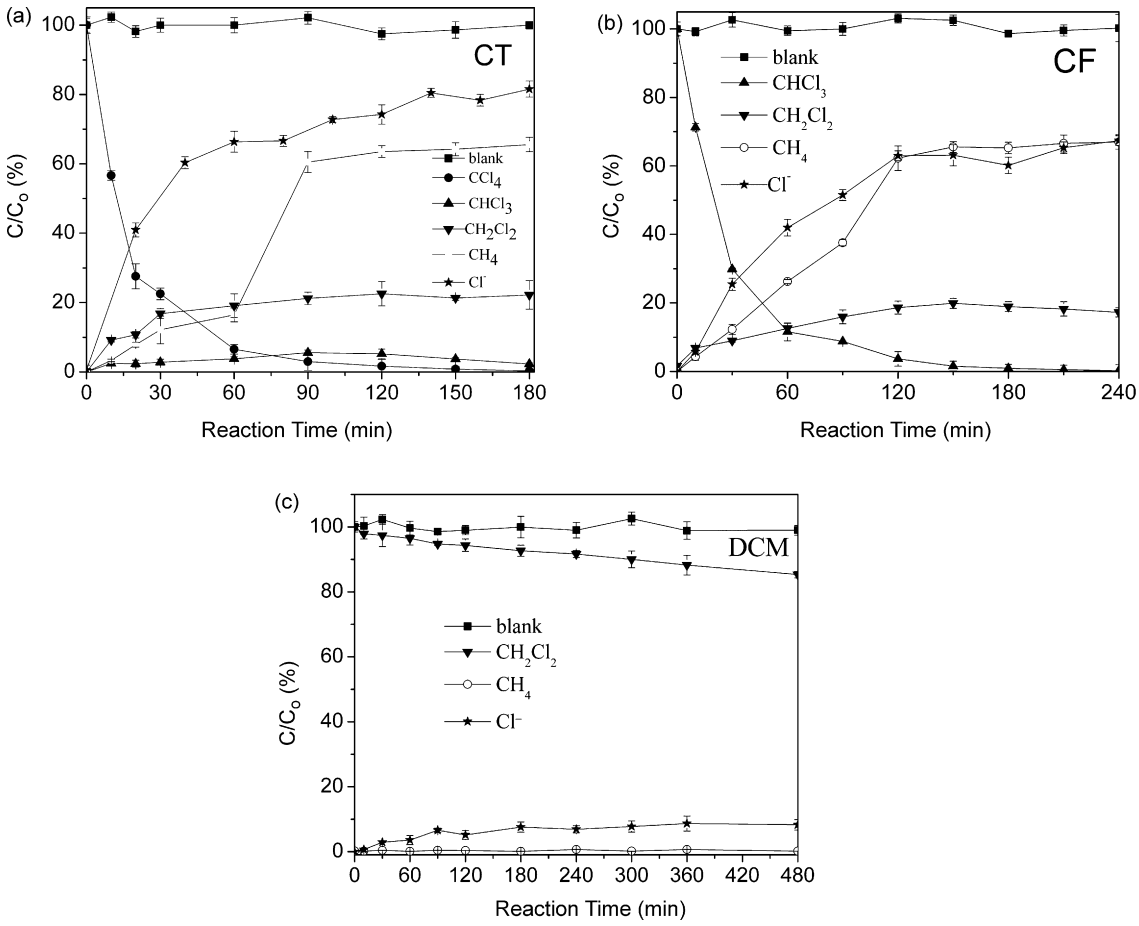

Fig. 10. Reaction of chlorinated methanes dechlorination by Pd/Fe bimetallic nanoparticles (Pd loading was 0.20 wt%, Pd/Fe addition was 10 g/L, and initial concentration of chlorinated methane was 100 mg/L).

nanoparticle surface and the presence of intermediates such as DCM led to the result that not all of the CF was dechlorinated within 240 min.

Fig. 10(c) illustrates the slight decline of the DCM concentration as time continued. The measured methane of reaction was a small amount, and about 15% of the initial DCM was transformed within 480 min. The decrease of initial DCM concentration might involve both adsorption and dechlorination. Burris et al. had testified that most intermediates of polychlorinated organic compound adhered to the Pd/Fe bimetallic particle surface during the process of dechlorination. Only a small amount of intermediates departed from the particles surface after being dechlorinated one chloride. As a result, the production of intermediate was detected in small amounts [2]. The low yield of chlorinated intermediates is an obvious advantage for the utility of Pd/Fe bimetallic nanoparticles.

3.4. Reaction kinetics of chlorinated methanes dechlorination by Pd/Fe bimetallic nanoparticles

The dechlorination of chlorinated methanes is a multistep reaction. The rate of transformation for CT, CF and DCM in a batch system was treated by a pseudo-first-order equation (Eq. (12)). Observed reaction rate constant (k_{obs}) is the measured rate constant. The natural logarithm of C/C_0 as a function of time for chlorinated methanes is shown in Fig. 11 (R^2 denotes square of fitting line correlation coefficient). The logarithmic plots versus time were linear ($R^2 > 0.97$). The slope of the line in Fig. 11 is k_{obs}. The surface-area-normalized rate coefficient (k_{SA}) is obtained using the following equations:

$$\ln\left(\frac{C}{C_0}\right) = -k_{obs}t \tag{12}$$

$$k_{obs} = k_{SA}a_s\rho_m \tag{13}$$

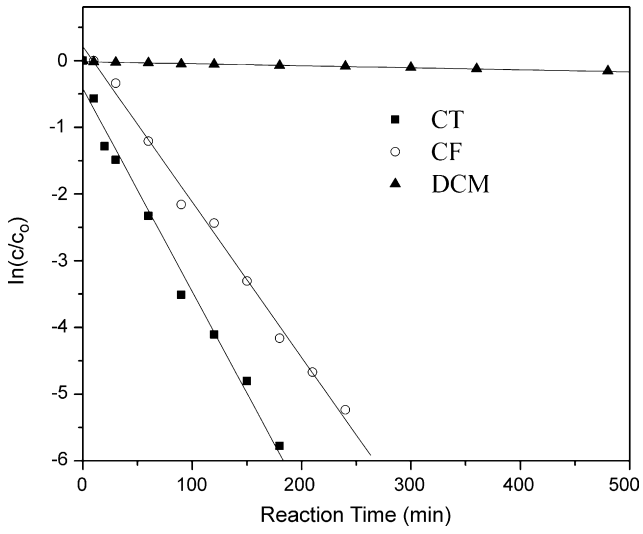

Fig. 11. Correlation for $\ln(C/C_0)$ and reaction time.

Table 1
k_{obs}, k_{SA}, $t_{1/2}$, and R^2 values for catalytic dechlorination of chlorinated methanes

Chlorinated methanes	k_{obs} (1/min)	k_{SA} (L/min m^2)	$t_{1/2}$ (min)	R^2
CT	3.080×10^{-2}	5.992×10^{-5}	22.50478	0.9719
CF	2.285×10^{-2}	4.446×10^{-5}	30.33467	0.9943
DCM	3.03×10^{-4}	5.895×10^{-7}	2333.043	0.9798

where a_s is the specific surface area (=51.4 m^2/g), and ρ_m is the Pd/Fe addition (=10 g/L). The calculation results are summarized in Table 1. In comparing different chlorinated levels, the dechlorination rate decreased with a decreasing number of chlorine atoms in the chlorinated methane molecule.

The following standard potentials (ΔE) for reduction of chlorinated methanes with elemental iron (pH 7, 25 °C) were calculated by Helland et al. [44].

$$Fe^0 + CCl_4 + H^+ \rightarrow Fe^{2+} + CHCl_3 + Cl^-, \qquad \Delta E = 1.11\,V$$

$$Fe^0 + CHCl_3 + H^+ \rightarrow Fe^{2+} + CH_2Cl_2 + Cl^-, \qquad \Delta E = 1.00\,V$$

$$Fe^0 + CH_2Cl_2 + H^+ \rightarrow Fe^{2+} + CH_3Cl + Cl^-, \qquad \Delta E = 0.93\,V$$

$$Fe^0 + CH_3Cl + H^+ \rightarrow Fe^{2+} + CH_4 + Cl^-, \qquad \Delta E = 0.91\,V$$

The above variation in standard potential might be a theoretical explanation of the result that the dechlorination rates of chlorinated methanes followed the order of CT > CF > DCM.

4. Conclusion

The catalytic dechlorination of chlorinated methanes by Pd/Fe bimetallic nanoparticles is effective and feasible. The advantages of Pd/Fe bimetallic nanoparticles for dechlorination are an expended surface area of particles, enhanced reactivity, and low concentration of intermediates. The dechlorination efficiencies of chlorinated methanes followed the order of CT > CF > DCM. The Pd loading, Pd/Fe addition, and initial pH value affected the dechlorination efficiency. The dechlorination efficiency increased with the increase of Pd/Fe addition. The optimal Pd loading and initial pH value for chlorinated methane dechlorination was 0.2 wt% and 7, respectively. The reactions were found to be pseudo-first-order with respect to chlorinated methane loss over time.

Acknowledgements

The authors are appreciative for the support of Program for Changjiang Scholars and Innovative Research Team in University (PCSIRT), the Ministry of Education and Scientific Research Foundation of Harbin Institute of Technology. Insightful comments and suggestions provided by three anonymous reviewers are profoundly acknowledged.

References

[1] I. Dror, M. Schlautman, Cosolvent effect on the catalytic reductive dechlorination of PCE, Chemosphere 57 (2004) 1505–1514.
[2] D.R. Burris, T.J. Campbell, V.S. Manoranjan, Sorption of trichloroethylene and tetrachloroethylene in a batch reactive metallic iron-water system, Environ. Sci. Technol. 29 (1995) 2850–2855.
[3] R.W. Gillham, S.F. O'Hannesin, Enhanced degradation of halogenated aliphatics by zero-valent iron, Ground Water 32 (1994) 958–967.
[4] L.J. Matheson, P.G. Tratnyek, Reductive dehalogenation of chlorinated methanes by iron metal, Environ. Sci. Technol. 28 (1994) 2045–2053.
[5] R. Muftikian, Q. Fernando, N. Korte, A method for the rapid dechlorination of low molecular weight chlorinated hydrocarbons in water, Water Res. 29 (1995) 2434–2439.
[6] W.X. Zhang, C.B. Wang, H.L. Lien, Treatment of chlorinated organic contaminants with nanoscale bimetallic particles, Catal. Today 40 (1998) 387–395.
[7] Y.H. Liu, F.L. Yang, P.L. Yue, G.H. Chen, Catalytic dechlorination of chlorophenols in water by palladium/iron, Water Res. 35 (2001) 1887–1890.
[8] N.E. Korte, J.L. Zutman, R.M. Schlosser, L. Liang, B. Gu, Q. Fernando, Field application of palladized iron for the dechlorination of trichloroethene, Waste Manage. 20 (2000) 687–694.
[9] J.L. Chin, L.L. Shang, H.L. Ya, Dechlorination of trichloroethylene in aqueous solution by noble metal-modified iron, J. Hazard. Mater. B 116 (2004) 219–228.
[10] C. Grittini, M. Malcomson, Q. Fernando, N. Korte, Rapid dechlorination of polychlorinated biphenyls on the surface of a Pd/Fe bimetallic system, Environ. Sci. Technol. 29 (1995) 2898–2900.
[11] J.L. Chen, R.A.S.R. A-Abed, J.A. Ryan, Z.B. Li, Effect of pH on dechlorination of trichloroethylene by zero-valent iron, J. Hazard. Mater. B 83 (2001) 243–254.
[12] H.L. Lien, W.X. Zhang, Transformation of chlorinated methanes by nanoscale iron particles, J. Environ. Eng. 125 (1999) 1042–1047.
[13] I.F. Cheng, Q. Fernando, N. Korte, Electrochemical dechlorination of 4-chlorophenol to phenol, Environ. Sci. Technol. 31 (1997) 1074–1078.
[14] J.T. Nurmi, P.G. Tratnyek, V. Sarathy, D.R. Baer, J.E. Amonette, K. Pecher, C. Wang, J.C. Linehan, D.W. Matson, R.L. Penn, M.D. Driessen, Characterization and properties of metallic iron nanoparticles: spectroscopy, electrochemistry, and kinetics, Environ. Sci. Technol. 39 (2005) 1221–1230.
[15] C.B. Wang, W.X. Zhang, Synthesizing nanoscale iron particles for rapid and complete dechlorination of TCE and PCBs, Environ. Sci. Technol. 31 (1997) 2154–2156.
[16] H.L. Lien, W.X. Zhang, Hydrodechlorination of chlorionated ethanes by nanoscale Pd/Fe bimetallic particles, J. Environ. Eng. 131 (2005) 4–10.
[17] W.S. Orth, R.W. Gillham, Dechlorionation of trichloroethene in aqueous solution using Fe^0, Environ. Sci. Technol. 30 (1996) 66–71.
[18] R.M. Hozalski, L. Zhang, W.A. Arnold, Reduction of haloacetic acids by Fe^0: implications for treatment and fate, Environ. Sci. Technol. 35 (2001) 2258–2263.
[19] J. Farrell, M. Kason, N. Melitas, T. Li, Investigation of the long-term performance of zero-valent iron for reductive dechlorination of trichloroethylene, Environ. Sci. Technol. 34 (2000) 514–521.
[20] T. Dombek, E. Dolan, J. Schultz, D. Klarup, Rapid reductive dechlorination of atrazine by zero-valent iron under acidic conditions, Environ. Pollut. 111 (2001) 21–27.
[21] H. Song, E.R. Carraway, Reduction of chlorinated methanes by nano-sized zero-valent iron. Kinetics, pathways, and effect of reaction conditions, Environ. Eng. Sci. 23 (2006) 272–284.
[22] H.L. Lien, Y.S. Jhuo, L.H. Chen, Effect of heavy metals on dechlorination of carbon tetrachloride by iron nanoparticles, Environ. Eng. Sci. 24 (2007) 21–30.
[23] J. Feng, T.T. Lim, Iron-mediated reduction rates and pathways of halogenated methanes with nanoscale Pd/Fe: analysis of liner free energy relationship, Chemosphere 66 (2007) 1765–1774.
[24] S. Choe, S.H. Lee, Y.Y. Chang, K.Y. Hwang, J. Khim, Rapid reductive destruction of hazardous organic compounds by nanoscale Fe^0, Chemosphere 42 (2001) 367–372.
[25] G.Y. Lowry, K.M. Johnson, Congener-specific dechlorination of dissolved PCBs by microscale and nanoscale zerovalent iron in a water/methanol solution, Environ. Sci. Technol. 38 (2004) 5208–5216.
[26] S.H. Joo, R.J. Feitz, T.D. Waite, Oxidative degradation of the carbothioate herbicide, molinate, using nanoscale zero-valent iron, Environ. Sci. Technol. 38 (2004) 2242–2247.
[27] H.L. Lien, W.X. Zhang, Nanoscale iron particles for complete reduction of chlorinated ethenes, Colloid Surf. A 191 (2001) 97–105.
[28] T.L. Johnson, M.M. Scherer, P.G. Tratnyek, Kinetics of halogenated organic compound degradation by iron metal, Environ. Sci. Technol. 30 (1996) 2640–2643.
[29] B.L. Cushing, V.L. Kolesnichenko, C.J. O'Connor, Recent advances in the liquid-phase syntheses of inorganic nanoparticles, Chem. Rev. 104 (2004) 3893–3946.
[30] N. Ichinose, Superfine Particle Technology, Spring-Verlag, Berlin, 1992.
[31] D.M. Cox, R.O. Brickman, K. Creegan, A. Kaldor, in: R.S. Averback, J. Bernholc, D.L. Nelson (Eds.), Clusters and Cluster-Assembled Materials, Materials Research Society, Pittsburgh, PA, 1991, p. 43.
[32] H.L. Lien, W.X. Zhang, Nanoscale Pd/Fe bimetallic particles: catalytic effects of palladium on hydrodechlorination, Appl. Catal. 77 (2007) 110–116.
[33] M. Nutt, J.B. Hughes, M. Wong, Designing Pd-on-Au bimetallic nanoparticle catalysis for trichloroethene hydrodechlorination, Environ. Sci. Technol. 39 (2005) 1343–1353.
[34] J. Yang, J.Y. Lee, L.X. Chen, H.P. Too, A phase-transfer identification of core-shell structures in Ag–Pt nanoparticles, J. Phys. Chem. B 109 (2005) 5468–5472.
[35] S. Mandal, P. Selvakannan, R. Pasricha, M. Sastry, Keggin ions as UV-switchable reducing agents in the synthesis of Au core–Ag shell nanoparticles, J. Am. Chem. Soc. 125 (2003) 8440–8441.
[36] Y. Xu, W.X. Zhang, Subcolloidal Fe/Ag particles for reductive dehalogenation of chlorinated benzenes, Ind. Eng. Chem. Res. 39 (2000) 2238–2244.
[37] K. Mondal, G. Jegadeesan, S.B. Lalvani, Removal of selenate by Fe and NiFe nanosized particles, Ind. Eng. Chem. Res. 43 (2004) 4922–4934.

[38] X.H. Xu, H.Y. Zhou, P. He, D.H. Wang, Catalytic dechlorination kinetics of *p*-dichlorobenzene over Pd/Fe catalysts, Chemosphere 58 (2005) 1135–1140.
[39] M.J. Alowitz, M.M. Scherer, Kinetics of nitrate, nitrite, and Cr(VI) reduction by iron metal, Environ. Sci. Technol. 36 (2002) 299–306.
[40] P.M. Jeffers, L.M. Ward, L.M. Woytowitch, N.L. Wolfe, Homogeneous hydrolysis rate constants for selected chlorinated methanes, ethanes, ethenes, and propanes, Environ. Sci. Technol. 23 (1989) 965–969.
[41] L.J. Graham, G. Jovanovic, Dechlorination of *p*-chlorophenol on a Pd/Fe catalyst in a magnetically stabilized fluidized bed: implications for sludge and liquid remediation, Chem. Eng. Sci. 54 (1999) 3085–3093.
[42] L.J. Graham, Dechlorination of *p*-chlorophenol on bimetallic Pd/Fe catalyst in a magnetically stabilized fluidized bed: experiment and theory, Ph.D. Thesis, Oregon State University, Corvallis, Oregon, 1999.
[43] N.J. Goran, Z.P. Polona, S. Ploenpun, A.K. Khaled, Dechlorination of *p*-chlorophenol in a microreactor with bimetallic Pd/Fe catalyst, Ind. Eng. Chem. Res. 44 (2005) 5099–5106.
[44] B.R. Helland, P.J.J. Alvarez, J.L. Schnoor, Reductive dechlorination of carbon tetrachloride with elemental iron, J. Hazard. Mater. 41 (1995) 205–216.

Glossary

SEM: scanning electron microscope
EDS: energy disperse X-ray spectroscopy
BET: Brunauer–Emmett–Teller
XRD: X-ray power diffraction
TEM: transmission electron microscope
COCs: chlorinated organic compounds
DCM: dichloromethane
CF: chloroform
CT: carbon tetrachloride
PTFE: polytetrafluorethylene
IC: ion chromatography.
GC: gas chromatograph
ECD: electron capture detector
FID: flame ionization detector
Pd loading: weight ratio of Pd to Fe
Pd/Fe addtion: Pd/Fe bimetallic nanoparticles to solution ratio